

Decompositional Quantum Graph Neural Network

Xing Ai,¹ Zhihong Zhang,² Luzhe Sun,³ Junchi Yan,⁴ Edwin Hancock,⁵

¹ Xiamen University, ² Xiamen University, ³ Xiamen University, ⁴ Shanghai Jiao Tong University, ⁵ University of York
Aixing1996@126.com, zhihong@xmu.edu.cn, 2627073690@qq.com,
yanjunchi@cs.sjtu.edu.cn, edwin.hancock@york.ac.uk

Abstract

Quantum machine learning is a fast emerging field that aims to tackle machine learning using quantum algorithms and quantum computing. Due to the lack of physical qubits and an effective means to map real-world data from Euclidean space to Hilbert space, most of these methods focus on quantum analogies or process simulations rather than devising concrete architectures based on qubits. In this paper, we propose a novel hybrid quantum-classical algorithm for graph-structured data, which we refer to as the Decompositional Quantum Graph Neural Network (DQGNN). DQGNN implements the GNN theoretical framework using the tensor product and unity matrices representation, which greatly reduces the number of model parameters required. When controlled by a classical computer, DQGNN can accommodate arbitrarily sized graphs by processing substructures from the input graph using a modestly-sized quantum device. The architecture is based on a novel mapping from real-world data to a Hilbert space. This mapping maintains the distance relations present in the data and reduces information loss. Experimental results show that the proposed method outperforms competitive state-of-the-art models with only 1.68% parameters compared to those models.

Introduction

Quantum machine learning encapsulates a diverse variety of algorithms ranging from classical shallow learning techniques such as the Quantum Support Vector Machine (QSVM) (Havlíček et al. 2019; Schuld and Killoran 2018) and the quantum decision tree classifier (Lu and Braunstein 2014) to the more recent quantum neural networks e.g. the Quantum Convolutional Neural Network (QCNN) (Cong, Choi, and Lukin 2019), the Quantum Generative Adversarial Network (QGAN) (Hu et al. 2019) and the Quantum Graph Neural Network (Verdon et al. 2019). Despite the progress in developing the quantum RNN (Bausch 2020) and QCNN (Cong, Choi, and Lukin 2019), the quantum version of the Graph Neural Network (GNN) (Scarselli et al. 2008) for real-world graph data has still not been well formulated or developed. In fact, the GNN has become an increasingly popular learning tool, especially for dealing with non-Euclidean data (Miller, Bliss, and Wolfe 2010). Emerging models and techniques include neighbor aggregation (Xu et al. 2018;

Veličković et al. 2018) which has found wide applications in social network analysis (Hamilton, Ying, and Leskovec 2017), drug design (Sun et al. 2020), combinatorial optimization (Khalil et al. 2017) and multi-agent learning (Liu et al. 2020). A quantum approach to the realization of GNN is therefore both conceptually attractive and an imperative for dealing with large-scale graphs with high efficiency.

Based on the above motivation, in this paper, we aim to develop a quantum GNN model with effective and scalable learning and a viable inference scheme. Specifically, we propose a Decompositional Quantum Graph Neural Network (DQGNN) whose efficacy is verified on graph classification.

Distinct from the Euclidean data usually processed by existing classical machine learning techniques, including deep learning, the data that must be processed in quantum machine learning resides in high-dimensional Hilbert spaces represented in the form of quantum states. It has been shown (Maria and Schuld 2019) that high-dimensional Hilbert space is beneficial to classification. Moreover, the aforementioned quantum machine learning methods have shown promising results. However, they are limited by the number of available physical qubits and lack a generic mapping method from the raw input data to the required quantum states.

GNNs are deep learning approaches that handle graph-structured data. The key idea underpinning GNNs is the neighborhood aggregation strategy. This involves updating the representation of a graph node by recursively aggregating the representations of its neighbors. Different realisations of the GNN include but are not limited to Relational Graph Convolutional Networks (R-GCN) (Schlichtkrull et al. 2018a), Graph Isomorphism Networks (GIN) (Jaume et al. 2019), edGNN (Xu et al. 2018), Random Walk Graph Neural Networks (RW-GNN) (Nikolentzos and Vazirgiannis 2020) and Factorizable Graph Convolutional Networks (Factor GCN) (Yang et al. 2020). However, these approaches embed nodes represents as points in a Euclidean space, which is not suitable for processing hierarchy graphs. Computations have undertaken in the Euclidean space lead to significant structural distortion and information loss (Chami et al. 2019).

Inspired by the above methods, this paper proposes a hybrid classical-quantum machine learning approach to Graph Neural Network embodiment. Compared to the existing quantum algorithm for graph-structured data (Verdon et al. 2019), our method is scale-free and able to utilize the features of

nodes. Additionally, we ground the GNN framework in the physical elements of quantum computing, i.e. qubits. Our main contributions are summarized as follows:

- 1) A novel quantum-classical hybrid machine learning algorithm for graph-structured data is proposed, namely Decompositional Quantum Graph Neural Network (DQGNN), which utilizes tensor product and unitary matrices to implement GNN theoretical framework. Due to the unitary matrix only needs a control rotation angle, i.e. variational parameter, DQGNN achieves similar performance with only 1.68% parameters compared with the least parameters GNN model, DGCNN (Zhang et al. 2018).
- 2) We design a decompositional processing strategy and provide experiment results to show the effectiveness of this strategy. By exploiting this strategy, the DQGNN can handle larger-sized graph-structured data with a fixed-sized quantum device, via the efficient use of qubits. In the current situation where the number of physical qubits is limited, this is an important feature of our method.
- 3) A trainable method for mapping data from a Euclidean space to a Hilbert space is proposed. It can maintain distance relations and reduces information loss during the mapping.

Related Work

We review two related topics, graph neural network and quantum machine learning.

The goal of graph neural networks is to map both node features and structural arrangement information to vectorized representations that can be used to embed graphs into lower-dimensional spaces and manifolds. Since the seminal work in (Scarselli et al. 2008), a varied set of GNN models have been proposed. For example, it has been proven (Xu et al. 2018) that a GNN that satisfies certain restrictive conditions can be as powerful as the Weisfeiler-Lehman (WL) test (Weisfeiler and Leman 1968) and can effectively distinguish the isomorphism of graphs. Mathematically it has been proved that GNNs can achieve the same effect as the WL test when three critical functions of the GNN satisfy are injective. This analysis has been further extended to directed graphs by aggregating nodes and edges at the same time (Jaume et al. 2019). The Fast and Deep Graph Neural Networks (FDGNN) (Gallicchio and Micheli 2020) makes it is possible to combine the advantages of the deep architectural construction of GNN’s with the extreme efficiency of randomized NN, and in particular RC, methodologies. Random Walk Graph Neural Network (RW-GNN) (Nikolentzos and Vazirgiannis 2020) generates graph representations by comparing a set of trainable ‘hidden graphs’ against the input graphs using a variant of the P -step random walk kernel.

Quantum Machine Learning (QML) brings quantum algorithms and quantum computing theory to machine learning. Unlike quantum algorithms which pursue exponential acceleration for specific problems (Debnath et al. 1991; Shor 1999), methods such as QCNN (Schlichtkrull et al. 2018b) and QGAN (Hu et al. 2019) aim to expand the embedding space of machine learning to quantum space, so as to achieve better performance. Although most of the existing QML models can not accelerate the calculation, they can be applied to a variety

of problems, such as classification (Li, Song, and Wang 2021), combinatorial optimization (Khairy et al. 2020) and so on. Seeking quantum counterparts of the Support Vector Machine (SVM) (Vapnik and Chervonenkis 1964), the work (Havlíček et al. 2019) proposes a quantum binary classification algorithm similar to SVM (QSVM). The Quantum Convolutional Neural Network (QCNN) (Schlichtkrull et al. 2018b) simulates the structure of the Convolutional Neural Network. For input sizes of N qubits, the QCNN has only $O(\log N)$ variational parameters. Quantum Generative Adversarial Network (QGAN) is developed in (Hu et al. 2019). It is shown that after rounds of training, the generator of the QGAN can generate the corresponding quantum states with high fidelity. (Schuld, Sweke, and Meyer 2021) theoretically prove that there exist quantum models that can approximate any functions if the accessible frequency spectrum is asymptotically rich enough, which shows the expression potential of quantum computing. Likely, (Schuld et al. 2020) propose a novel quantum model that encoding several copies of a data vector by utilizing quantum devices to achieve higher polynomial degrees separation boundaries. These models have been successfully applied to perform classification tasks in a Hilbert space. However, two main problems limit their applicability to large-scale real-world data. Firstly, there is a lack of general methods to map data to quantum states. Secondly, due to the limited number of available qubits, high-dimensional data can not be easily loaded into QML algorithms.

To overcome these shortcomings, we propose a novel hybrid quantum-classical¹ machine learning method which we refer to as the Decompositional Quantum Graph Neural Network (DQGNN). Specifically, it utilizes unitary weight matrices and the tensor product to embed the node representation into a Hilbert space, to satisfy the injective mapping condition (Xu et al. 2018) required by the graph classification task. We will prove this mathematically in the following section. As a result, DQGNN achieves comparable performance with classical GNNs but the parameters of our model are only 1.68% of the classical counterpart. Besides, a novel decompositional processing is designated, which is applicable to high-dimensional structural data and can work with small number of available qubits (only one qubit in our experiments) on real-world data as the model gradually processes the whole graph by decomposing it into multiple subgraphs.

Methodology

In this paper, we develop a novel quantum-classical hybrid machine learning algorithm for graph-structured data. The idea is to develop a quantum GNN by designing a quantum circuit and replacing the Euclidean weight matrices of the GNN with unitary matrices, i.e. quantum gates. In this way, we incorporate theoretical ideas from quantum machine learning into deep learning in the graph domain.

In this section, we first introduce the theoretical framework underpinning our model and provide the mathematical proofs. Then, we introduce the quantum circuit to implement

¹Note that most QML methods (Havlíček et al. 2019; Schuld and Killoran 2018; Schlichtkrull et al. 2018b; Hu et al. 2019) are in fact all quantum-classical hybrids.

DQGNN, the trainable mapping method and the sequential decompositional processing strategy. Finally, we introduce the structure of QGNN and explain how the DQGNN can be used to classify quantum states and then summarize the processes underpinning DQGNN.

Theoretical Framework of DQGNN

To distinguish graph isomorphisms by quantum machine learning, we follow the study of Xu et al. (Xu et al. 2018), and introduce the theoretical framework GNNs using quantum machine learning. What makes GNN so powerful is its injective aggregation strategy, which maps different nodes to different representational units. As a result, different graphs have different representations.

The GNN model (Xu et al. 2018) can be represented by:

$$\mathbf{h}_v^k = \sigma \left(\mathbf{h}_v^{(k-1)} \mathbf{W}_1^{(k-1)} + \sum_{\mu \in \mathcal{N}(v)} \mathbf{h}_\mu^{(k-1)} \mathbf{W}_2^{(k-1)} \right) \quad (1)$$

here \mathbf{h}_v^t is the representation of node v at the representation of t -th iteration and $\mathcal{N}(v)$ is the neighbor set of node v . The matrices $\mathbf{W}_1^{(k-1)}$ and $\mathbf{W}_2^{(k-1)}$ are respectively trainable weight matrices at the $(k-1)$ -th layer for node v and its neighbors. The σ is network activation function.

The aim of this paper is to provide a route to implementing Eq. 1 on a quantum computer. For quantum computing, the state of a physical system composed of several qubits is obtained by a tensor product of the individual qubit quantum states, namely quantum entanglement. The tensor product is one of the fundamental constructs of quantum computing. Due to the ability to enlarge the space exponentially, the tensor product can be used to map different nodes to different representations. The tensor product is analogous to the summation operation in classical GNNs. In other words, both the tensor product and the summation are injective functions.

Lemma 1. *The tensor product is injective, for non-zero vectors with the same dimension. As a result, the tensor product maps them to different representations unless they are linearly dependent vectors.*

All the proofs including that for this Lemma can be found in the Appendix. Since quantum states are complex vectors, according to Lemma 1, the tensor product maps different quantum states to different representations. Moreover, all quantum states are linearly independent.

Lemma 2. *If two quantum states \mathbf{A} and \mathbf{B} are linearly dependent, and $\mathbf{B} = k \cdot \mathbf{A}$, then $k = \pm 1$.*

Due to the property of quantum states, Lemma 2 can be demonstrated easily using the proof in the Appendix. According to Lemma 1 and Lemma 2, the tensor product maps two quantum states to the same representation if and only if the two quantum states are identical.

So, for the DQGNN, the tensor product replaces the summation of the GNN, and Eq. 1 becomes:

$$\mathbf{h}^{t-1}(v) \rightarrow |\varphi_v\rangle^{t-1}, \quad \mathbf{h}^{t-1}(\mu) \rightarrow |\varphi_\mu\rangle^{t-1} \quad (2)$$

$$|\varphi_v\rangle^t = \mathbf{U}_1 |\varphi_v\rangle^{t-1} \otimes \left(\bigotimes_{\mu \in \mathcal{N}(v)} \mathbf{U}_2 |\varphi_\mu\rangle^{t-1} \right) \quad (3)$$

$$\mathbf{h}^t(v) = -\text{tr}(\rho^t \log \rho^t), \quad \rho^t = |\varphi_v\rangle^t \langle \varphi_v|^t \quad (4)$$

where \mathbf{U}_1 and \mathbf{U}_2 are unitary matrices with trainable parameters, which correspond to the Euclidean weight matrices \mathbf{W}_1 and \mathbf{W}_2 in the GNN of Eq. 1. Unlike the weight matrices of classical GNN which have many numerical parameters to train, the unitary matrices have only a single variational parameter which represents rotation angles of the quantum states. Details on unitary matrices and their properties are given in Appendix.

Note Eq. 3 implements on a quantum computer and returns the result to a classical computer. We will discuss the implementation of Eq. 3 in next section. Eq. 2 is achieved by the proposed mapping method. The representation of the next layer can be obtained by von Neumann entropy in Eq. 4.

Both Eq. 1 and Eq. 3 are able to distinguish non-isomorphic graphs, i.e. graph classification. To demonstrate the effectiveness of the DQGNN for the graph isomorphism problem, we need to prove that Eq. 3 will map nodes with different features or neighbors to different representations.

Lemma 3. *For different nodes v and μ , the outputs of Eq. 3: $|\varphi_v\rangle$ and $|\varphi_\mu\rangle$, meet $|\varphi_v\rangle \neq |\varphi_\mu\rangle$.*

A natural follow-up theorem is that the DQGNN can distinguish graphs that are decided as non-isomorphic graphs by the GNNs based on Eq. 1.

Theorem 1. *DQGNN maps two non-isomorphic graphs G_1 and G_2 as decided via GNN by Eq. 3 to different embeddings.*

Compared with the GNN, the main differences of the DQGNN are the tensor product aggregation operator and the unitary matrix. The advantages of using tensor product and unitary matrix are as follows:

1) The tensor product enlarges the node representation space exponentially. As a result, nodes with different features can be mapped to different representations. Although alternative other functions such as the dot product and matrix multiplication are both injective functions, their implementations on quantum devices are not as convenient as the tensor product, because the tensor product is a fundamental facet of quantum computing.

2) Since the tensor product can enlarge the representation space exponentially, DQGNN has significantly fewer parameters than related deep learning models. A layer of the GNN requires a $d \times h$ weight matrix to transform a d -dimensional input into a h -dimensional output. Such a layer has $d \times h$ parameters that need to be trained. For DQGNN, the entanglement of $\max(\log_2 d, \log_2 h)$ qubits can generate $\max(d, h)$ -dimension quantum states. DQGNN has only $n \cdot \max(\log_2 d, \log_2 h)$ variational parameters for training if n quantum gates are applied to each qubit, because a unitary matrix has only one variational parameter (the rotation of the quantum states).

Quantum Circuit of our DQGNN

To implement Eq. 3 on a quantum device, we design a quantum circuit with a hierarchical structure similar to the GNNs. The quantum circuit we have designed contains K Ulayers to capture the information within the K -hop neighbours of a

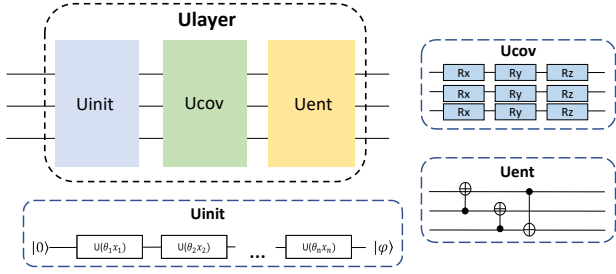


Figure 1: Ulayer with Uinit, Ucov, and Uent.

node. A Ulayer includes three components: Uinit, Ucov and Uent. As shown in Fig. 1. For n nodes input, the initial states of the quantum circuit are $|0\rangle^{\otimes n}$. The output is the tensor product of the quantum states overall qubits.

We allocate a quantum circuit and the requisite qubits to the subgraph consisting of a node and its neighbours. After the required computations have completed, we then free the quantum circuit and its qubits.

The Uinit component maps the data to quantum states, which corresponds to the quantum circuit of the trainable mapping method mentioned later in this section. Specifically, it is responsible for mapping node features from Euclidean space to Hilbert space. The Ucov component, on the other hand, has three quantum gates on each qubit: **RX**, **RY**, **RZ**. Each quantum gate accepts one trainable parameter. All neighbours of a node share parameters but not include the node. For arbitrary qubit of the Ucov component, if the input quantum state is $|\varphi_{in}\rangle$, the output is $|\varphi_{out}\rangle$:

$$|\varphi_{out}\rangle = \mathbf{U}_{cov}|\varphi_{in}\rangle = \mathbf{RX}(\theta_x)\mathbf{RY}(\theta_y)\mathbf{RZ}(\theta_z)|\varphi_{in}\rangle \quad (5)$$

The \mathbf{U}_{cov} corresponds to \mathbf{U}_1 or \mathbf{U}_2 in Eq. 3. $\theta_x, \theta_y, \theta_z$ are variational parameters of quantum gates. The output of Ulayer is a tensor product over the quantum states of all nodes, corresponding to $|\varphi_v\rangle^t$ in Eq. 3. Therefore, the Ulayer component implements Eq. 3. In a manner similar to the GNN, the DQGNN can aggregate features of the k -hop neighbours to a node by applying K Ulayers. The Ucov is followed by a Uent component, which applies a CNOT gate to each pair of qubits to entangle their information.

The parameters of the Uinit component have been trained and will not be updated during the training of Ulayer.

Trainable Mapping Method

Existing quantum machine learning techniques (Havlíček et al. 2019; Hu et al. 2019; Rebentrost, Mohseni, and Lloyd 2014; Cong, Choi, and Lukin 2019; Lloyd and Weedbrook 2018; Situ et al. 2020) is mainly applied to artificial data or small-scale real-world data. One reason for this restriction is due to the lack of an effective mapping from a variety of real-world data to quantum states. To address this problem, we propose a trainable mapping to maintain the distances between data to reduce information loss of mapping.

Quantum states are distributed on the surface of the Bloch sphere that resides in Hilbert space. Mapping data in Euclidean space to the Bloch sphere may incur a large distortion, as shown in Fig. 2.

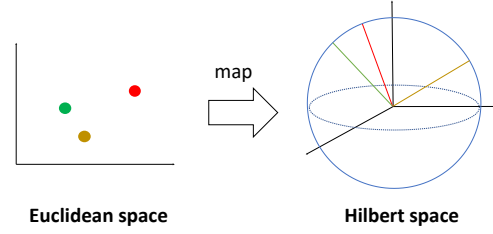


Figure 2: In Euclidean space, the distance between the green point and the orange one is smaller than that between the green and the red. After mapping the data points to Hilbert space, points close to each other in Euclidean space become more distant in quantum states (the green and orange lines), while the distance between the points which are farther away in Euclidean space becomes closer (the red and green lines).

The distance relations between the quantum states on the Bloch sphere are expected to be consistent with those between the data in Euclidean space. Any two sample points that are close to each other in Euclidean space should also be close after the mapping to Hilbert space. If this is not the case, the distance difference between the quantum states and the data will induce information loss and impair the subsequent analysis operations. Considering the above problem, we present a mapping method in which the loss is related to the difference in the distance relations between the Euclidean space and the Bloch sphere. The corresponding circuit implementation for this method is shown in the Uinit component of Fig. 1. For n -dimensional data $\mathbf{x} = (x_1, x_2, \dots, x_n)$, the mapping circuit repeatedly uses a qubit with n quantum gates to map each sample to corresponding quantum state. Each quantum gates accepts the product of x_i and the trainable parameter θ_i as parameter. Obviously, the Euclidean distance is not suitable for distance measurement on the Bloch sphere, which is a unit sphere. We utilize the inverse cosine of the inner product of the quantum states for distance measure. The reason why we chose inverse cosine is the low computational complexity and natural consistency with the spherical representation. We believe other non-Euclidean distance measures are also available for our model, e.g. hyperbolic distances.

We construct a loss based on the correlation matrix \mathbf{D} and \mathbf{D}' of the data and the corresponding quantum states:

$$\mathbf{D}'_{ij} = \frac{\arccos(\langle\varphi_i|\varphi_j\rangle)}{\max(\mathbf{D}')}, \quad L_{map} = \sum_{i=1}^n \sum_{j=1}^n |\mathbf{D}_{ij} - \mathbf{D}'_{ij}| \quad (6)$$

where \mathbf{D}_{ij} is the normalized Euclidean distance between samples i and j . Similarly \mathbf{D}'_{ij} is the normalized distance defined in Eq. 6 between quantum state i and j .

Compared with the existing mapping methods of quantum algorithms, the main difference of the proposed mapping method is applying trainable parameters to maintain the distance relationships between data and quantum states which reduces the information loss. Our experiments will show the effectiveness of our method.

Decompositional Processing Strategy

One bottleneck for quantum machine learning is the lack of available physical qubits in handling real-world data.

Algorithm 1: Decompositional processing for graph

Input: $G = (V, E)$, $|V| = N$; node features $X = \{x_v | \forall v \in V\}$.

Output: subgraph set $\{S_v | \forall v \in V\}$, subgraph features set $\{C_v | \forall v \in V\}$.

```
1: for  $v \in V$  do
2:   add  $v$  and  $N(v)$  to  $S_v$ ;
3:   for  $\mu \in N(v)$  do
4:     add  $X_\mu$  to  $C_v$ ;
5:   end for
6: end for
```

For efficient use of qubits, we propose a decompositional processing strategy via subgraph decomposition. Concretely, according to Eq. 1 and Eq. 3, the iterative updating of the representation of node v is obtained by aggregating node v together with its neighbors $N(v)$ from the current iteration. As a result, the iterative updating of each node in a graph is only related to its neighbors. Therefore, we regard a node and its neighbours as a subgraph. A graph containing N nodes can be decompositional into N subgraphs. DQGNN computes the representation of each subgraph sequentially. As such, the process only requires a fixed number of qubits.

To commence, the entire graph is divided into several subgraphs using a classical computer. The number of subgraphs is equal to the number of nodes. Next, the quantum circuits process each subgraph sequentially and return the representation of each subgraph to the classical computer. Finally, the subgraph representations are re-merged to reconstitute the original graph representation using the classical computer.

For a graph with N nodes, the number of qubits required to compute its representation is accordingly reduced from N to D by introducing the above subgraph decomposition, where D is the maximum degree of the graph. If the number of available qubits $n < D$, we can divide the neighbour sets $\mathcal{N}(v)$ of node v into M sets: $\mathcal{N}(v) = \mathcal{N}_1(v) \cup \mathcal{N}_2(v) \cup \dots \cup \mathcal{N}_m(v)$. All sets meet conditions:

$$|\mathcal{N}_i(v)| \leq n, \quad \mathcal{N}_i(v) \cap \mathcal{N}_j(v) = \emptyset, \quad i, j \in [1, m], i \neq j \quad (7)$$

We sequentially compute the representations of the sets:

$$|\varphi_{v_i}\rangle^{t-1} = \bigotimes_{\mu \in \mathcal{N}_i(v)} \mathbf{U}_2 |\varphi_\mu\rangle^{t-1} \quad (8)$$

$$|\varphi_v\rangle^t = \mathbf{U}_1 |\varphi_v\rangle^{t-1} \bigotimes_{i \in [1, m]} \left(\bigotimes_{\mu \in \mathcal{N}_i(v)} |\varphi_{v_i}\rangle^{t-1} \right), \quad i \in [1, m] \quad (9)$$

Eq. 9 is computed using the classical computer, as $|\varphi_{v_i}\rangle^{t-1}$ is stored in the classical computer.

For the effectiveness of the decompositional processing strategy, we provide the following results.

Theorem 2. For the same inputs, Eq. 9 is equivalent to Eq. 3.

We provide the proof of this theorem in Appendix.

Structure of DQGNN

The output of quantum circuit is a tensor product over the quantum states of all nodes, giving a high-dimensional vector. To classify graphs, the von Neumann entropy is summed over

Algorithm 2: Trainable mapping for quantum representation

Input: input features $X = \{x_v \in \mathbb{R}^d | \forall v \in V\}$, random initial parameters of mapping circuit $P \in \mathbb{R}^d$, the mapping circuit MC .

Output: trained initial parameters of mapping circuit $P_t \in \mathbb{R}^d$.

```
1: for  $i \in V$  do
2:   for  $j \in V$  do
3:      $\mathbf{D}_{ij} = x_i \cdot x_j$ ;
4:   end for
5: end for
6: for  $i \in V$  do
7:    $|\varphi_i\rangle \leftarrow MC(P, x_i)$ ;
8: end for
9: for  $i \in V$  do
10:  for  $j \in V$  do
11:     $\mathbf{D}'_{ij} = \arccos(\langle \varphi_i | \varphi_j \rangle)$ ;
12:     $L_{map} = L_{map} + |\mathbf{D}_{ij} - \mathbf{D}'_{ij}|$ ;
13:  end for
14: end for  $P_t = \underset{P}{\operatorname{argmin}} Loss$ ;
```

quantum states of all nodes as a characterization of the graph.

The classical Shannon entropy measures the uncertainty associated with a classical probability distribution for a set of data. Quantum states can be described in a similar way using density operators in place of probability distributions, and the von Neumann entropy in place of the Shannon entropy. For a system with pure quantum state $|\varphi_i\rangle$ the density matrix is $\rho = \sum_i |\varphi_i\rangle \langle \varphi_i|$, and the graph representation \mathbf{h}_G is:

$$\mathbf{h}_G = \sum_{v \in G} S(\rho_v), \quad \rho_v = |\varphi_v\rangle \langle \varphi_v| \quad (10)$$

$$S(\rho_v) = -\operatorname{tr}(\rho_v \log \rho_v) \quad (11)$$

For the binary classification problem, the Quantum Support Vector Machine (QSVM) (Havlíček et al. 2019) classifies data by measuring components of quantum states along the Pauli-Z direction. The quantum states on the upper Bloch hemisphere are assigned to one class and the quantum states on the lower Bloch hemisphere are assigned to the other class. Our approach is essentially the same as QSVM. We use two quantum states corresponding to two classes, and these correspond to the upper and lower Bloch hemispheres. The von Neumann entropies of two quantum states are ρ_0 and ρ_1 . Suppose \mathbf{h}_G is the representation of graph G to be classified, the label y_G of graph G is:

$$y_G = \begin{cases} 0, & \text{if } |\rho_0 - \mathbf{h}_G| \geq |\rho_1 - \mathbf{h}_G| \\ 1, & \text{else} \end{cases} \quad (12)$$

More details about the training of the DQGNN are given in the Appendix. DQGNN consists of the following processing steps, where K is the number of iterations.

Step 1) Classic computer decomposes graph to subgraphs.

Step 2) Train the circuit of the mapping method with node features. The trained parameters of the circuit are stored on a classical computer. After training, the node features of the subgraphs are mapped into quantum states by applying the circuit.

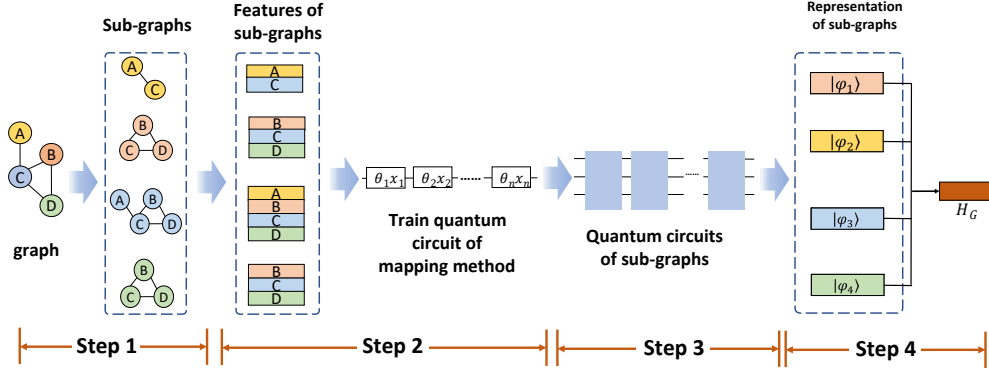


Figure 3: An instance of the DQGNN. Step 1 and Step 4 are implemented on classical computer. The quantum circuits of Step 2 and Step 3 can run on quantum circuit or simulator of classical computer.

Algorithm 3: Framework of our DQGNN

Input: subgraph set $\{S_v | \forall v \in V\}$ with features $\{C_v | \forall v \in V\}$, the quantum circuit of DQGNN mentioned in Sec. QC , Predefined von Neumann entropies of two classes: ρ_0 and ρ_1 .

Output: label prediction for graph G : l_G .

- 1: **for** $v \in V$ **do**
 - 2: $|\varphi_v\rangle \leftarrow QC(S_v, C_v);$
 $\rho_v = |\varphi_v\rangle\langle\varphi_v|;$
 - 3: **end for**
 - 4: $\mathbf{h}_G = \sum_{v \in V} \rho_v;$
 - 5: $y_G = \begin{cases} 0, & \text{if } |\rho_0 - \mathbf{h}_G| \geq |\rho_1 - \mathbf{h}_G|; \\ 1, & \text{else} \end{cases}$
-

Step 3) The quantum device runs the quantum circuit to compute the representations of the different subgraphs sequentially. The classical computer stores all the representations computed in this way.

Step 4) A classical computer computes the entropies of the individual representations and combines them by Eq. 11.

Step 5) Steps 1-4 are repeated to obtain graph representations for classification. Fig. 3 shows the structure.

Summary of the DQGNN Framework

We summarize the framework of DQGNN, whose decompositional processing strategy is shown in Alg. 1, which corresponds to step 1 of Fig. 3, as running on a classic computer. While Alg. 2 involves step 2 of Fig. 3. After training, Alg. 2 outputs the initial parameters of the mapping circuit. Step 3 and step 4 of Fig. 3 are summarized in Alg. 3, whose output is the input graph assigned label.

Experiments

We evaluate DQGNN on six graph classification benchmarks. The compared methods include graph kernels, deep learning methods and quantum machine learning methods. Detailed descriptions of the datasets, the experimental protocol and experiments on synthetic data, together with additional relevant information are in the appendix.

Baselines for Comparison

To the best of our knowledge, there are no quantum machine learning methods for graph data that can be used for the purposes of direct comparison. So, we apply QSVM (Havlíček et al. 2019) and QCNN (Cong, Choi, and Lukin 2019) to graph data. Due to the limitations imposed by the number of qubits, high-dimensional graph data cannot be handled by QSVM and QCNN directly. Fortunately, Yanardag et al. (Yanardag and Vishwanathan 2015) proposed a dimension reduction method to encode high-dimensional graph to low-dimensional representation based on the number of graphlets. They define eight typical motifs that can capture the local information of the graph and calculate their information entropy which is an 8-dimensional vector. Therefore, we use this method to encode a high-dimensional graph into an 8-dimensional vector, and then use the 8-dimensional vector as the input of QSVM and QCNN. Additionally, we compare DQGNN with recent baselines for graph classification:

- 1) Kernel based methods: WL subtree kernel (Shervashidze et al. 2010) and Subgraph Matching Kernel (CSM) (Kriege and Mutzel 2012).
- 2) Representative GCNs, including Deep Graph CNN’s (DGCNN) (Zhang et al. 2018) and Relational Graph Convolutional Networks (R-GCN) (Schlichtkrull et al. 2018a).
- 3) Representative GNNs, i.e., Graph Isomorphism Network (GIN) (Jaume et al. 2019), edGNN (Xu et al. 2018), RW-GNN (Nikolentzos and Vazirgiannis 2020).

Experimental Setup

We use three Ulayers in DQGNN for all of our experiments. The Ulayers have identical structure but independent parameters. During the training, UOBYQA (Powell 2002) based on a derivative-free optimization method is chosen for training DQGNN. The quantum machine learning models are all run on a quantum simulator on a classical computer. The computer code used for QSVM are provided by Qiskit (Bozso-Rey and Loredó 2018), and the codes for QCNN are from Tensorflow Quantum (Broughton et al. 2021). For the classical GNN models, the source code comes from the authors publicly available implementations. The performances for classical GNNs are quoted from the indicated reference. We perform 10-fold cross-validation to compute accuracies on

Table 1: Evaluation for graph classification accuracy over six benchmarks (in % \pm standard error).

Datasets	MUTAG	PTC_FM	PTC_FR	PTC_MM	PTC_MR	PROTEINS
WL (Shervashidze et al. 2010)	90.4 \pm 5.7	60.4	65.7	66.6	59.9 \pm 4.3	75.0 \pm 3.1
CSM (Kriege and Mutzel 2012)	85.4	63.8	65.5	63.3	58.1	-
DGCNN (Zhang et al. 2018)	85.8	57.31 \pm 4.2	63.5 \pm 3.9	60.96 \pm 8.4	58.6	70.9 \pm 2.8
R-GCN (Schlichtkrull et al. 2018a)	81.5	60.7	65.8	64.7	58.2	-
edGNN (Xu et al. 2018)	86.9	59.8	65.7	64.4	56.3	-
GIN (Jaume et al. 2019)	89.4 \pm 5.6	64.28 \pm 10.0	65.34 \pm 5.6	65.82 \pm 5.9	64.6 \pm 7.0	76.2 \pm 2.8
RW-GNN (Nikolentzos and Vazirgiannis 2020)	89.2 \pm 4.3	61.03 \pm 1.5	63.02 \pm 2.1	63.08 \pm 1.9	56.10 \pm 1.2	74.7 \pm 3.3
Gra+QSVM (Havlíček et al. 2019)	81.80 \pm 10.3	60.66 \pm 5.4	62.50 \pm 10.2	57.50 \pm 8.8	60.89 \pm 7.3	71.10 \pm 6.6
Gra+QCNN (Cong, Choi, and Lukin 2019)	81.04 \pm 14.1	59.86 \pm 10.9	63.2 \pm 11.2	58.96 \pm 9.9	61.53 \pm 8.6	77.05 \pm 10.1
Gra+QCNN (w/ M) (Cong, Choi, and Lukin 2019)	81.88 \pm 9.3	61.88 \pm 3.5	64.8 \pm 4.11	61.25 \pm 5.53	62.02 \pm 3.3	78.9 \pm 7.8
DQGNN (w/o M)	82.28 \pm 10.53	60.35 \pm 6.4	64.40 \pm 9.4	60.71 \pm 2.2	62.84 \pm 8.3	70.51 \pm 5.6
DQGNN	85.83 \pm 3.7	64.57 \pm 4.6	67.3 \pm 5.6	65.67 \pm 2.5	65.14 \pm 5.6	79.78 \pm 4.7

PTC_FM, PTC_MM, PTC_FR. The parameters for the deep learning methods are as suggested by their authors. For fairness, all the methods run on the same computing device.

Results and Discussion

Table 1 reports the mean and std of the accuracy for graph classification obtained by 10-fold cross-validation. We also perform an ablation study without using our trainable mapping method (DQGNN (w/o M)) to verify its effectiveness.

Comparison with classic learning methods: Table 1 indicates that DQGNN achieves the best results on 5 out of 6 benchmarks, often with a clear improvement over peer classic GNN models. The accuracy of the DQGNN with trainable mapping on PTC_FM and PTC_MM are 64.57 ± 4.6 and 65.67 ± 2.5 respectively, which are closed to GIN with smaller standard error. For PTC_FR and PTC_MR, DQGNN achieves 1.5% and 0.54% improvements than the second-best methods. When DQGNN does not achieve the top performance, its accuracy is still close to that of the GNNs.

Comparison of parameters: As a result of using the tensor product and unitary matrices, DQGNN has fewer parameters than GNNs but achieves comparable performance, as shown in Table 2. Our DQGNN (w/o M) and DQGNN have 36 and 43 parameters respectively, which are both less than 2% of those of the recent quantum GNN model DGCNN (Zhang et al. 2018). Note that DGCNN has the least parameters among the different GNNs. Compared to other quantum machine learning models, e.g. QSVM (Havlíček et al. 2019) has 36 parameters and QCNN (Cong, Choi, and Lukin 2019) has 54 parameters. Note that the inputs of QSVM and QCNN are the results of dimension reduction.

Comparison with alternative quantum machine learning methods: Here, Gra+QSVM and Gra+QCNN in Table 1 refer to using the graphlet count vector as the inputs to QSVM and QCNN, respectively. QSVM has its mapping circuit shown in Appendix but QCNN hasn't. We apply the mapping circuits shown in Fig. 1 to QCNN (Gra+QCNN (w/ M)). The results of Gra+QSVM, Gra+QCNN and Gra+QCNN (w/ M) represent no improvement on DQGNN. Moreover, compared to Gra+QCNN, Gra+QCNN (w/ M) achieves higher accuracy. This demonstrates that our proposed trainable mapping method is also effective when combined with alternative quantum machine learning algorithms.

Comparison of DQGNN (w/o M) and DQGNN: We observe that DQGNN with our trainable mapping method slightly and consistently outperforms DQGNN without this

Table 2: Model parameter comparison. The parameters of GNN include all the parameters of the weight matrix to be trained, and the parameters of quantum algorithm are the angles required by all quantum gates (unitary matrix)

Model	Parameters
DGCNN (Zhang et al. 2018)	2560
R-GCN (Schlichtkrull et al. 2018a)	16704
edGNN (Xu et al. 2018)	9345
GIN (Jaume et al. 2019)	13000
QSVM (Havlíček et al. 2019)	36
QCNN (Cong, Choi, and Lukin 2019)	54
DQGNN (w/o M)	36
DQGNN	43

trainable mapping i.e. DQGNN (w/o M). Since they have the same structure, the improvement may be attributed by less information loss compared to the DQGNN without the mapping method. Note that the accuracy of DQGNN is about 9% higher than DQGNN (w/o M) on the PROTEINS, while for the MUTAG, the accuracy of DQGNN (w/o M) is close to that of DQGNN. Table 1 shows that the PROTEINS has 61 vertex labels while MUTAG has only seven. This means that PROTEINS requires higher dimension for node features and suffers more serious information loss. The results show that our trainable mapping method reduces information loss and improves performance. Besides, for most datasets, the standard error of DQGNN is less than DQGNN (w/o M). For example, the standard error of DQGNN (w/o M) and DQGNN on PTC_FR are respectively 9.4 and 5.6. When there is no trainable mapping, the elements of the node feature vector are used as the gate parameters to map data to quantum states. This leads to a random distribution of quantum states in the Hilbert space.

Conclusion

In this paper, we have presented a novel hybrid quantum-classical algorithm for graph structure data, namely the Decompositional Quantum Graph Neural Network (DQGNN). We introduce the framework of DQGNN originated from classic GNN and provide theoretical proof showing that our DQGNN can handle graph isomorphism problems. We also propose a decompositional processing involving subgraphs. Scalability issues relating to the number of qubits can be addressed only by processing a subgraph each time in DQGNN.

References

- Bausch, J. 2020. Recurrent Quantum Neural Networks. arXiv:2006.14619.
- Bozzo-Rey, M.; and Loredó, R. 2018. Introduction to the IBM Q experience and quantum computing. In *Proceedings of the 28th Annual International Conference on Computer Science and Software Engineering*, 410–412.
- Broughton, M.; Verdon, G.; McCourt, T.; Martínez, A. J.; Yoo, J. H.; Isakov, S. V.; Massey, P.; Halavati, R.; Niu, M. Y.; Zlokapa, A.; Peters, E.; Lockwood, O.; Skolik, A.; Jerbi, S.; Dunjko, V.; Leib, M.; Streif, M.; Dollen, D. V.; Chen, H.; Cao, S.; Wiersema, R.; Huang, H.-Y.; McClean, J. R.; Babbush, R.; Boixo, S.; Bacon, D.; Ho, A. K.; Neven, H.; and Mohseni, M. 2021. TensorFlow Quantum: A Software Framework for Quantum Machine Learning. arXiv:2003.02989.
- Chami, I.; Ying, Z.; Ré, C.; and Leskovec, J. 2019. Hyperbolic graph convolutional neural networks. In *Advances in neural information processing systems*, 4868–4879.
- Cong, I.; Choi, S.; and Lukin, M. D. 2019. Quantum convolutional neural networks. *Nature Physics*, 15(12): 1273–1278.
- Debnath, A. K.; Compadre, R. L. L. D.; Debnath, G.; Shusterman, A. J.; and Hansch, C. 1991. Structure-activity relationship of mutagenic aromatic and heteroaromatic nitro compounds. Correlation with molecular orbital energies and hydrophobicity. *Journal of Medicinal Chemistry*, 34(2): 786–797.
- Gallicchio, C.; and Micheli, A. 2020. Fast and deep graph neural networks. In *Proceedings of the AAAI Conference on Artificial Intelligence*, volume 34, 3898–3905.
- Hamilton, W.; Ying, Z.; and Leskovec, J. 2017. Inductive Representation Learning on Large Graphs. In Guyon, I.; Luxburg, U. V.; Bengio, S.; Wallach, H.; Fergus, R.; Vishwanathan, S.; and Garnett, R., eds., *Advances in Neural Information Processing Systems 30*, 1024–1034. Curran Associates, Inc.
- Havlíček, V.; Córcoles, A. D.; Temme, K.; Harrow, A. W.; Kandala, A.; Chow, J. M.; and Gambetta, J. M. 2019. Supervised learning with quantum-enhanced feature spaces. *Nature*, 567(7747): 209–212.
- Hu, L.; Wu, S.-H.; Cai, W.; Ma, Y.; Mu, X.; Xu, Y.; Wang, H.; Song, Y.; Deng, D.-L.; Zou, C.-L.; and Sun, L. 2019. Quantum generative adversarial learning in a superconducting quantum circuit. *Science Advances*, 5(1).
- Jaume, G.; phi Nguyen, A.; Martínez, M. R.; Thiran, J.-P.; and Gabrani, M. 2019. edGNN: a Simple and Powerful GNN for Directed Labeled Graphs. arXiv:1904.08745.
- Khairy, S.; Shaydulin, R.; Cincio, L.; Alexeev, Y.; and Balaprakash, P. 2020. Learning to optimize variational quantum circuits to solve combinatorial problems. In *Proceedings of the AAAI Conference on Artificial Intelligence*, volume 34, 2367–2375.
- Khalil, E. B.; Dai, H.; Zhang, Y.; Dilkina, B.; and Song, L. 2017. Learning Combinatorial Optimization Algorithms over Graphs. In *NIPS*.
- Kriege, N.; and Mutzel, P. 2012. Subgraph Matching Kernels for Attributed Graphs. *Proceedings of the 29th International Conference on Machine Learning, ICML 2012*, 2.
- Li, G.; Song, Z.; and Wang, X. 2021. VSQ: Variational Shadow Quantum Learning for Classification. In *Proceedings of the AAAI Conference on Artificial Intelligence*, volume 35, 8357–8365.
- Liu, Y.; Wang, W.; Hu, Y.; Hao, J.; Chen, X.; and Gao, Y. 2020. Multi-agent game abstraction via graph attention neural network. In *Proceedings of the AAAI Conference on Artificial Intelligence*, volume 34, 7211–7218.
- Lloyd, S.; and Weedbrook, C. 2018. Quantum Generative Adversarial Learning. *Physical Review Letters*, 121(4): 040502.1–040502.5.
- Lu, S.; and Braunstein, S. 2014. Quantum decision tree classifier. *Quantum information processing*, 3(13): 757–777.
- Maria; and Schuld. 2019. Machine learning in quantum spaces. *Nature*.
- Miller, B. A.; Bliss, N. T.; and Wolfe, P. J. 2010. Toward signal processing theory for graphs and non-Euclidean data. In *2010 IEEE International Conference on Acoustics, Speech and Signal Processing*, 5414–5417.
- Nikolentzos, G.; and Vazirgiannis, M. 2020. Random Walk Graph Neural Networks. *Advances in Neural Information Processing Systems*, 33: 16211–16222.
- Powell, M. J. D. 2002. UOBYQA: unconstrained optimization by quadratic approximation. *Mathematical Programming*, 92(3): 555–582.
- Rebentrost, P.; Mohseni, M.; and Lloyd, S. 2014. Quantum support vector machine for big data classification. *Physical Review Letters*, 113(13): 130503.
- Scarselli, F.; Gori, M.; Tsoi, A. C.; Hagenbuchner, M.; and Monfardini, G. 2008. The graph neural network model. *IEEE transactions on neural networks*, 20(1): 61–80.
- Schlichtkrull, M.; Kipf, T. N.; Bloem, P.; Van Den Berg, R.; Titov, I.; and Welling, M. 2018a. Modeling relational data with graph convolutional networks. In *European semantic web conference*, 593–607. Springer.
- Schlichtkrull, M.; Kipf, T. N.; Bloem, P.; van den Berg, R.; Titov, I.; and Welling, M. 2018b. Modeling Relational Data with Graph Convolutional Networks. In *15th International Conference on Extended Semantic Web Conference, ESWC 2018*, 593–607. Springer/Verlag.
- Schuld, M.; Bocharov, A.; Svore, K. M.; and Wiebe, N. 2020. Circuit-centric quantum classifiers. *Physical Review A*, 101(3): 032308.
- Schuld, M.; and Killoran, N. 2018. Quantum machine learning in feature Hilbert spaces. *Physical Review Letters*.
- Schuld, M.; Sweke, R.; and Meyer, J. J. 2021. Effect of data encoding on the expressive power of variational quantum-machine-learning models. *Phys. Rev. A*, 103: 032430.
- Shervashidze, N.; Schweitzer, P.; Jan, E.; Leeuwen, V.; and Borgwardt, K. M. 2010. Weisfeiler-Lehman Graph Kernels. *Journal of Machine Learning Research*, 1: 1–48.
- Shor, P. W. 1999. Polynomial-Time Algorithms for Prime Factorization and Discrete Logarithms on a Quantum Computer. *Siam Review*, 41(2): 303–332.

- Situ, H.; He, Z.; Wang, Y.; Li, L.; and Zheng, S. 2020. Quantum generative adversarial network for generating discrete distribution. *Information Sciences*, 538: 193–208.
- Sun, M.; Zhao, S.; Gilvary, C.; Elemento, O.; Zhou, J.; and Wang, F. 2020. Graph convolutional networks for computational drug development and discovery. *Briefings in bioinformatics*, 21(3): 919–935.
- Vapnik, V. N.; and Chervonenkis, A. 1964. A note on one class of perceptrons. *Automation and Remote Control*, 25.
- Veličković, P.; Cucurull, G.; Casanova, A.; Romero, A.; Liò, P.; and Bengio, Y. 2018. Graph Attention Networks. *International Conference on Learning Representations*.
- Verdon, G.; McCourt, T.; Luzhnica, E.; Singh, V.; Leichenauer, S.; and Hidary, J. 2019. Quantum Graph Neural Networks. arXiv:1909.12264.
- Weisfeiler, B.; and Leman, A. 1968. A reduction of a Graph to a Canonical Form and an Algebra Arising during this Reduction (in Russian). *Nauchno-Technicheskaya Informatsia*, 9.
- Xu, K.; Hu, W.; Leskovec, J.; and Jegelka, S. 2018. How Powerful are Graph Neural Networks? In *International Conference on Learning Representations*.
- Yanardag, P.; and Vishwanathan, S. 2015. Deep graph kernels. In *Proceedings of the 21th ACM SIGKDD international conference on knowledge discovery and data mining*, 1365–1374.
- Yang, Y.; Feng, Z.; Song, M.; and Wang, X. 2020. Factorizable Graph Convolutional Networks. *Advances in Neural Information Processing Systems*, 33.
- Zhang, M.; Cui, Z.; Neumann, M.; and Chen, Y. 2018. An end-to-end deep learning architecture for graph classification. In *Proceedings of the AAAI Conference on Artificial Intelligence*, volume 32.